Supplementary Information

Mechanistic Insight into Effect of Active Site Motif Structure on Direct Oxidation of Methane to Methanol over Cu-ZSM-5

Chengna Dai, Yuchan Zhang, Ning Liu,* Gangqiang Yu, Ning Wang, Ruinian Xu, Biaohua Chen

Faculty of Environment and Life, Beijing University of Technology, Beijing, 100124, China
*Correspondence to: liuning@bjut.edu.cn

Table of Content

Theoretical method of ab initio thermodynamics (AIT) analysis

The DFT-based ab initio thermodynamics (AIT) were conducted to evaluate the thermostabilities of diverse active site structures under the reaction condition of present work, including $[Cu]^+$, $[Cu\text{-}O]^+$, $[Cu]^+$--$[Cu]^+$, $[Cu\text{-}O\text{-}Cu]^{2+}$ and $[Cu\text{-}OH]^+$, according to the Eq. S1.

$$\frac{2m-n-2x-2y+i}{2}N_2O+\frac{n-i}{2}H_2O+yCuO+xFeO+H_i\text{-}Z$$
$$f\quad Fe_xCu_yO_mH_n\text{-}Z+\frac{2m-n-2x-2y+i}{2}N_2 \tag{S1}$$

The Gibbs free energy difference [ΔG(T,P)] can be calculated according to the Eq. S2:

$$\Delta G(T,p)=G_{Cu_yO_mH_n\text{-}Z}+\frac{2m-n-2x-2y+i}{2}\mu^g_{N_2}-$$
$$E_{H_i\text{-}Z}-yE_{CuO}-\frac{n-j}{2}\mu^g_{H_2O}-\frac{2m-n-2x-2y+i}{2}\mu^g_{N_2O} \tag{S2}$$

As noted, the bulk CuO as well as H-ZSM-5 (noted as H_i-Z) was calculated by DFT to derive the E_{CuO} and $E_{Hi\text{-}Z}$. As for other reference molecules of N_2, N_2O and H_2O, the related chemical potentials of $\mu^g_{N_2}$, $\mu^g_{N_2O}$ and $\mu^g_{H_2O}$ was employed in Eq.S2, which can be calculated according to the Eqs. S3-S8.

$$\mu^g_{N_2}(T,p)=E_{N_2}+\Delta\mu_{N_2}(T,p) \tag{S3}$$

$$\mu^g_{N_2O}(T,p)=E_{N_2O}+\Delta\mu_{N_2O}(T,p) \tag{S4}$$

$$\mu^g_{H_2O}(T,p)=E_{H_2O}+\Delta\mu_{H_2O}(T,p) \tag{S5}$$

$$\Delta\mu_{N_2}(T,p)=\Delta\mu_{N_2}(T,p^0)+RT\ln(\frac{p_{N_2}}{p^0_{N_2}}) \tag{S6}$$
$$=H(T,p^0,N_2)-H(0K,p^0,N_2)-T[S(T,p^0,N_2)-S(0K,p^0,N_2)]+RT\ln(\frac{p_{N_2}}{p^0_{N_2}})$$

$$\Delta\mu_{N_2O}(T,p)=\Delta\mu_{N_2O}(T,p^0)+RT\ln(\frac{p_{N_2O}}{p^0_{N_2O}}) \tag{S7}$$
$$=H(T,p^0,N_2O)-H(0K,p^0,N_2O)-T[S(T,p^0,N_2O)-S(0K,p^0,N_2O)]+RT\ln(\frac{p_{N_2O}}{p^0_{N_2O}})$$

$$\Delta\mu_{H_2O}(T,p)=\Delta\mu_{H_2O}(T,p^0)+RT\ln(\frac{p_{H_2O}}{p^0_{H_2O}}) \tag{S8}$$
$$=H(T,p^0,H_2O)-H(0K,p^0,H_2O)-T[S(T,p^0,H_2O)-S(0K,p^0,H_2O)]+RT\ln(\frac{p_{H_2O}}{p^0_{H_2O}})$$

The reaction energies of ΔE can be defined as

$$\Delta E=E_{Cu_yO_mH_n-z}+\frac{2m-n-2y+i}{2}E_{N_2}-E_{H_i\text{-}Z}-yE_{CuO}-\frac{n-i}{2}E_{H_2O}-\frac{2m-n-2x-2k+i}{2}E_{N_2O} \tag{S9}$$

Above all, the ΔG(T,P) can be calculated by Eq. S10:

$$\Delta G(T,p) = \Delta E - \frac{2\mathrm{m} - \mathrm{n} - 2\mathrm{x} - 2\mathrm{y} + \mathrm{i}}{2}[\Delta\mu_{\mathrm{N_2}}(T,P) - \Delta\mu_{H_2O}(T,P)] - \frac{\mathrm{n} - \mathrm{i}}{2}\Delta\mu_{\mathrm{H_2O}}(T,P) \quad \text{(S10)}$$

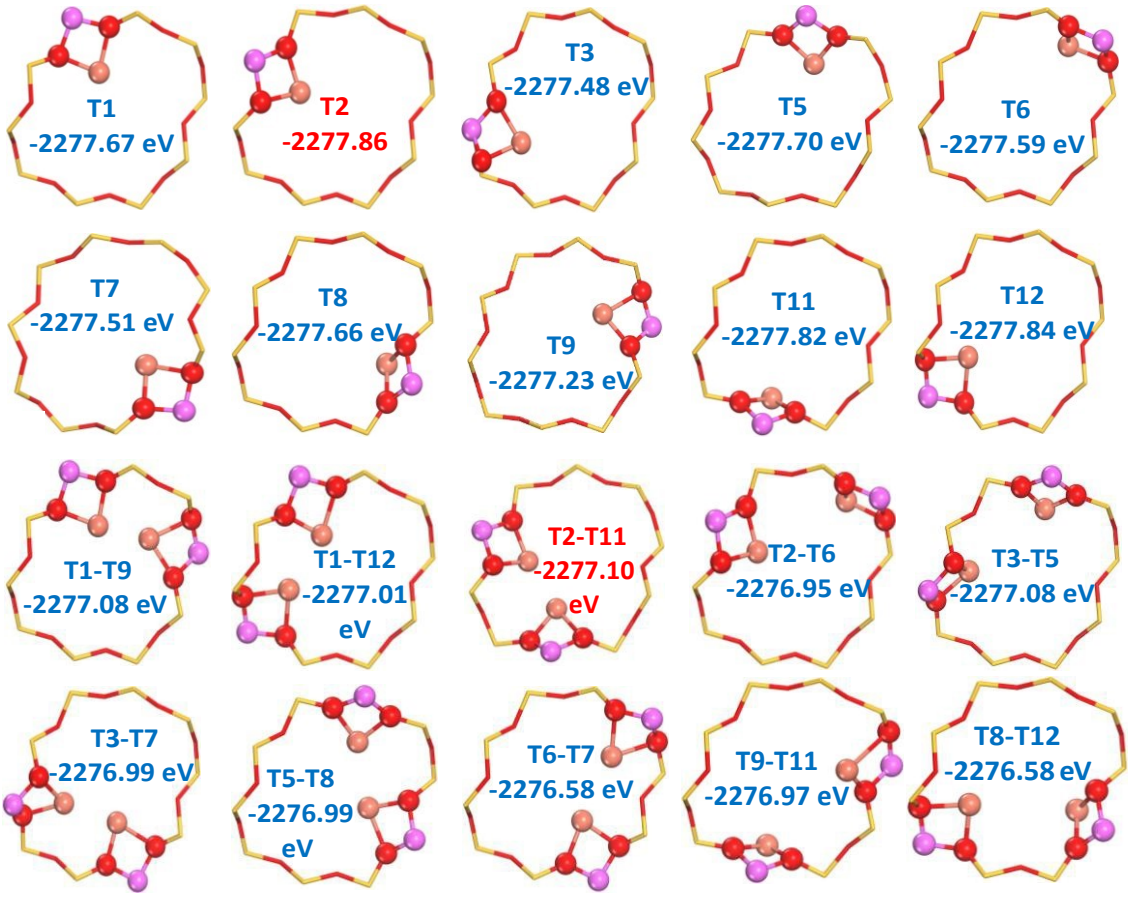

Fig. S1 Comparisons of DFT calculated energies for the Cu-ZSM-5 models with dicopper active sties being loaded at different T sites. The T2-T11 site was chose as the dicopper site model, which displays the lowest energy.

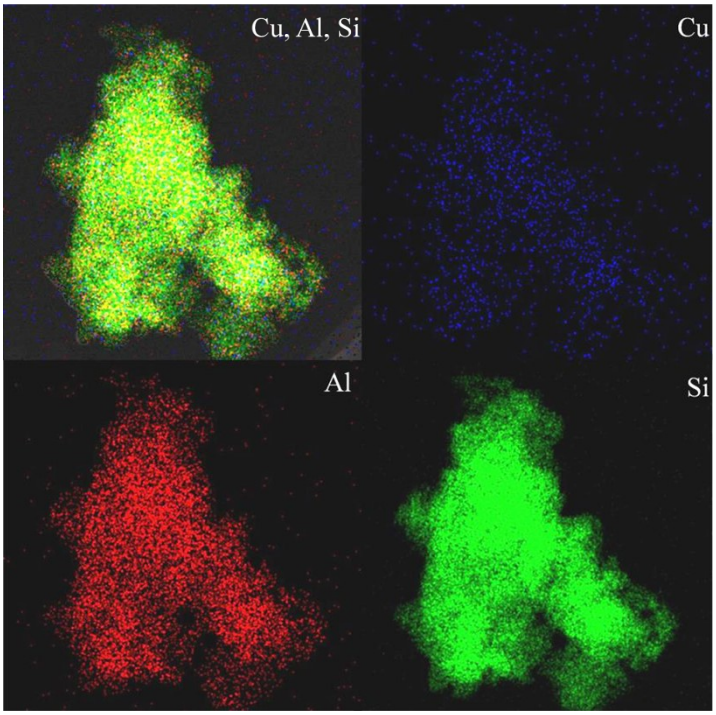

Fig. S2 TEM-EDX mapping results of elements Cu, Al and Si over Cu-ZSM5-0.3%; the well dispersion of Cu can be observed.

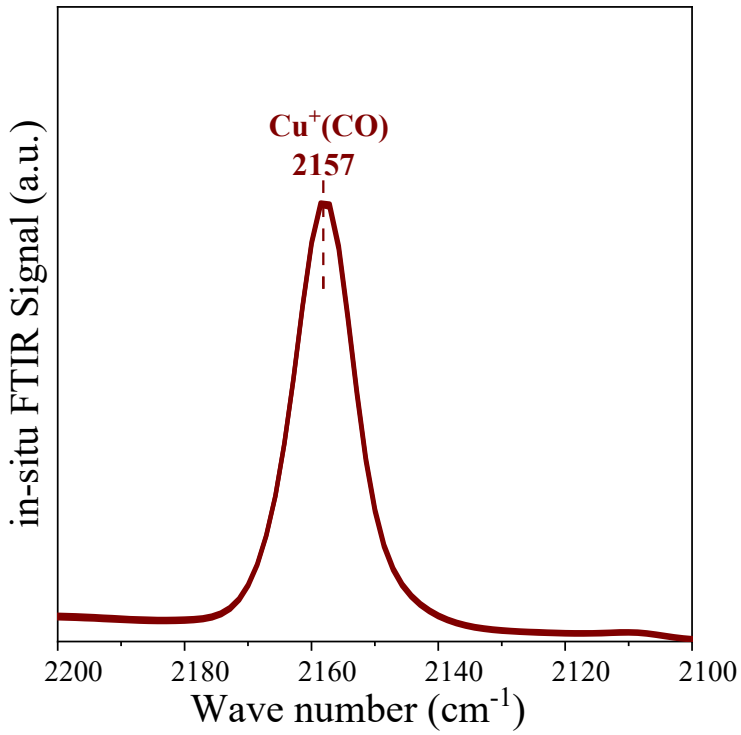

Fig. S3 Co-FTIR with the Cu-ZSM-5-0.3% being predated at *T* of 100 °C under vacuum condition for 30 min; and then the CO was introduced into the system with the signal being monitored at *T* of 50 °C.

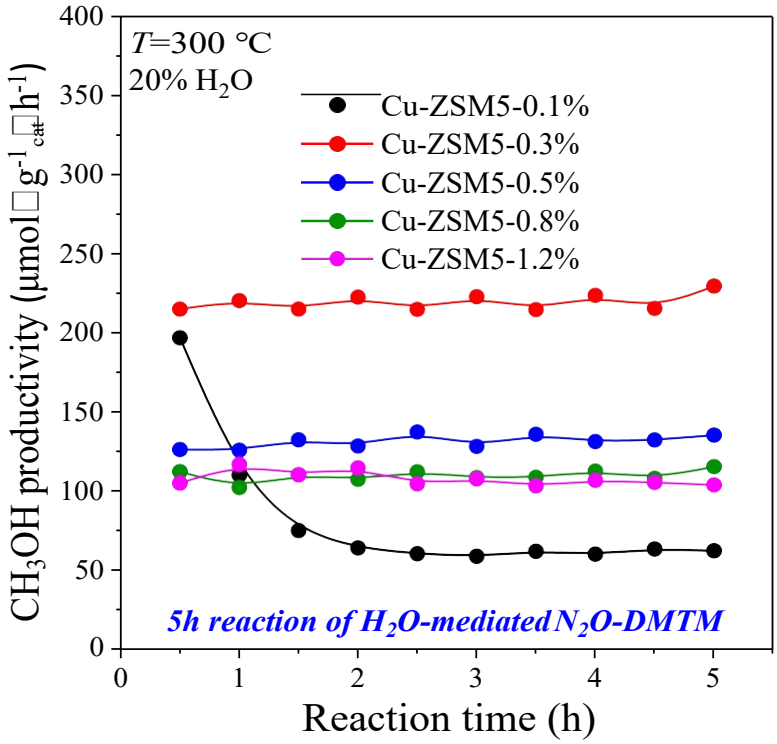

Fig. S4 Activity measurement results of H_2O mediated N_2O-DMTM over Cu-ZSM-5-n samples (n = 0.1, 0.3, 0.5, 0.8 and 1.2%) for 5 hours; reaction condition: N_2O: CH_4: H_2O: He= 30: 15: 20: 35; GHSV=12,000h^{-1}; T = 300 °C.

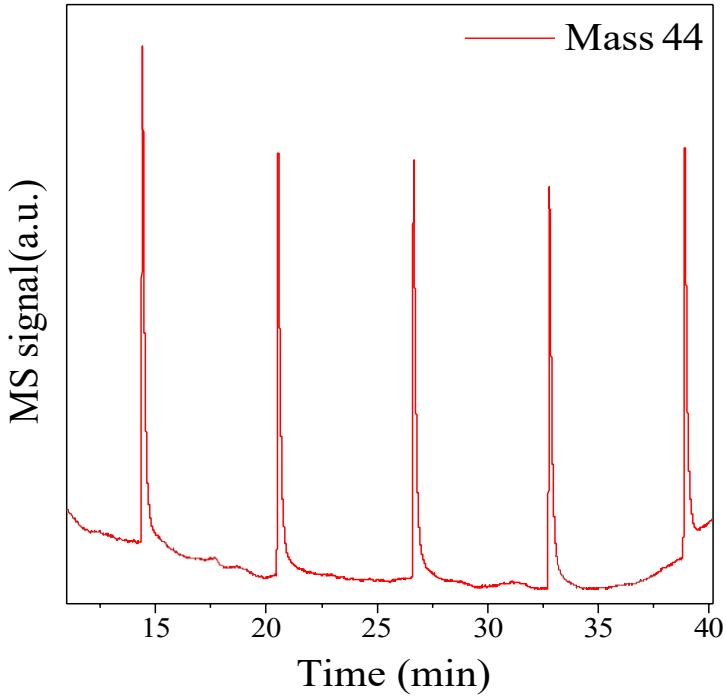

Fig. S5 Pulse test after bubbling the CH_3OH (~2 vol%, He of 40 mL min^{-1}) over CuO/SiO_2 at T = 300 °C and with the m/e signal of 44 (CO_2) being detected by mass spectrometer (MS).

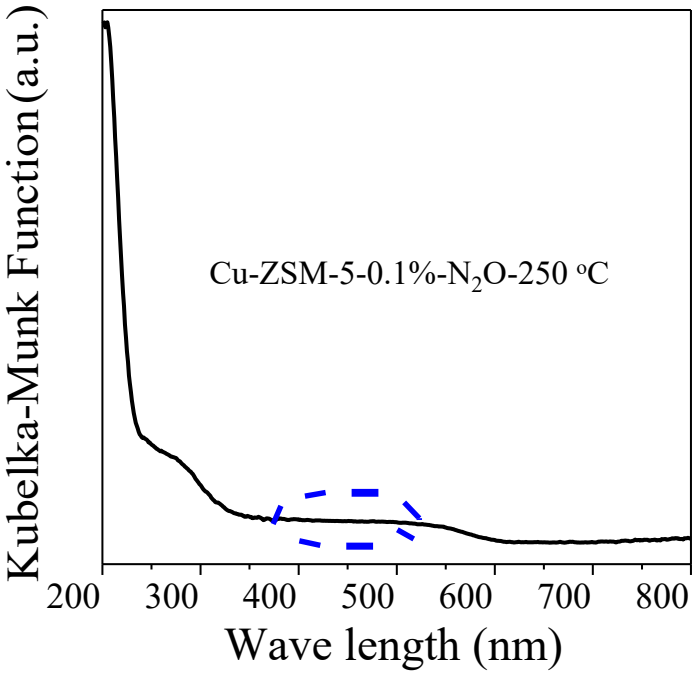

Fig. S6 UV-vis spectra of Cu-ZSM5-0.3% pretreated by N_2O at *T* of 250 °C; no peaks being related to $[Cu\text{-}O\text{-}Cu]^{2+}$ species can be observed around 440 nm.

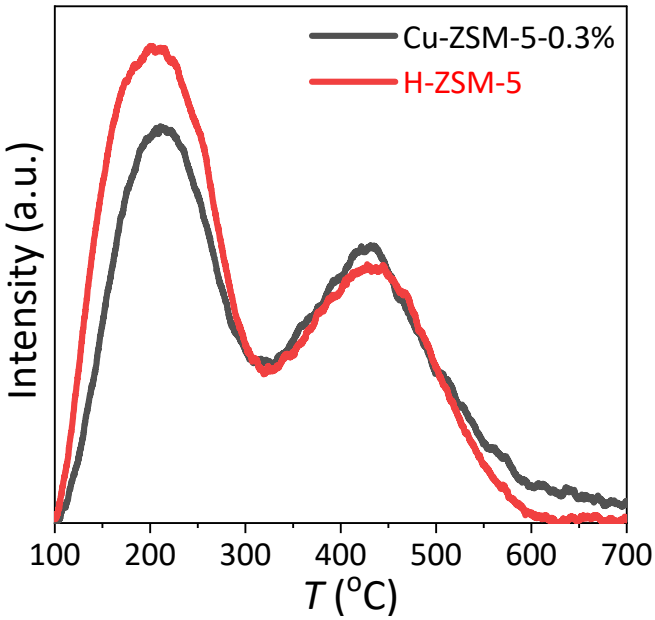

Fig. S7 NH_3-TPD results of pristine H-ZSM-5 and Cu-ZSM-5-0.3%

Note: Fig. S7 displays the NH_3-TPD of H-ZSM-5 and Cu-ZSM-5-0.3%. As can be seen, after the SSIE of Cu with H-ZSM-5, the acidity was slightly decreased from 0.82 to 0.68 mmol g^{-1} due to Cu loadings.

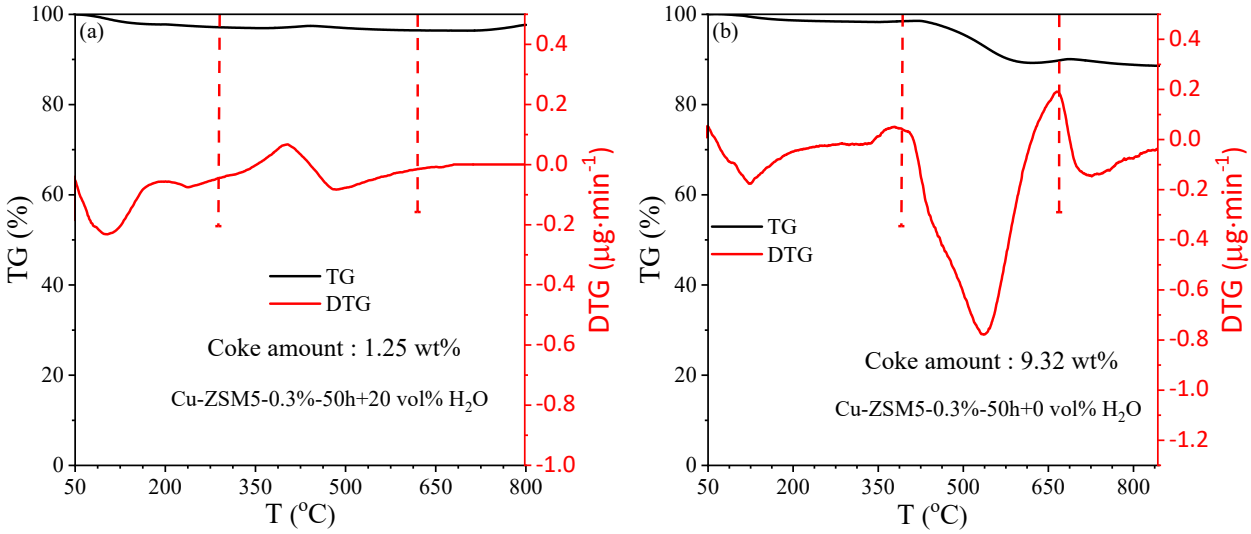

Fig. S8 Thermogravimetry (TG) and differential thermogravimetric analysis (DTG) curves of the Cu-BEA-0.3% samples being after long-term test in (a) presence and (b) absence of 20vol% H_2O.

Note: Figs. S8a-S8b display the TG results for the sample of Cu-ZSM-5 being after 50h's long-term reaction, in presence and absence of 20% H_2O. Much more extensive weight decreasing can be obviously found for the scenario of N_2O-DMTM in absence of H_2O, based on which the coke deposition amounts were estimated to be as high as 9.32 wt.%, with respect to 1.25 wt.% for the scenario of N_2O-DMTM in presence of 20 vol% H_2O.

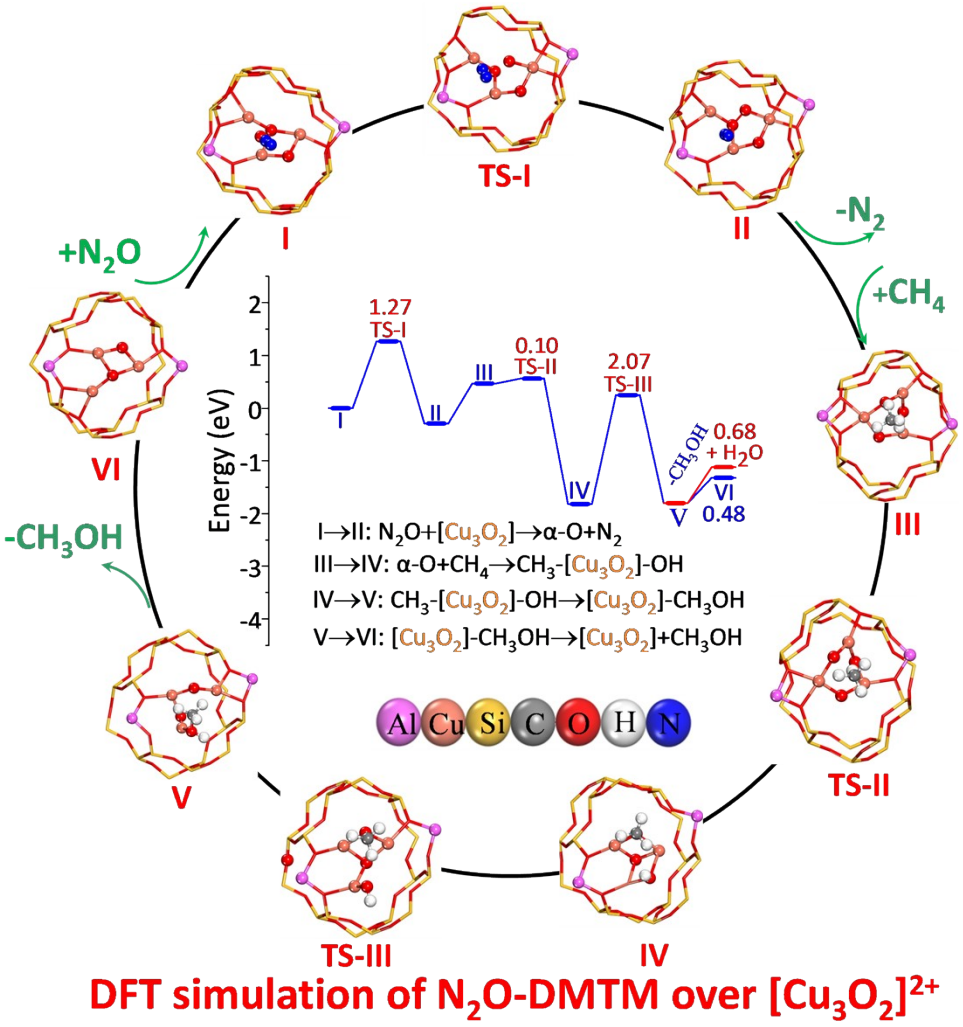

Fig. S9 Theoretical mechanism simulations of H_2O-mediated and H_2O-absence N_2O-DMTM by DFT over Cu-ZSM-5 with $[Cu_3O_2]^{2+}$ active site.

Table S1 Product selectivity during N_2O-DMTM over Cu-ZSM-5-n samples at *T* of 300 °C.

Samples	*T* (°C)	t (h)	Selectivity (%)						
			CO_2	C_2H_4	C_2H_6	C_3H_6	CH_3OH	C_2H_6O	Coke
Cu-ZSM5-0.3%	300	5	9.8	4.7	0.4	1.0	4.1	0.6	79.3
Cu-ZSM5-0.3%+10%H_2O	300	5	20.3	0.4	0	0	52.3	2.7	24.3
Cu-ZSM5-0.3%+30%H_2O	300	5	7.1	0.1	0	0	60.0	1.5	31.3
Cu-ZSM5-0.1%+20%H_2O	300	5	15.3	9.8	0.6	1.9	9.9	0.2	62.3
Cu-ZSM5-0.3%+20%H_2O	300	5	10.7	0.1	0	0	67.1	2.6	19.8
Cu-ZSM5-0.5%+20%H_2O	300	5	53.2	0	0	0	31.2	1.2	14.4
Cu-ZSM5-0.8%+20%H_2O	300	5	64.1	0	0	0	23.1	0.7	12.1
Cu-ZSM5-1.2%+20%H_2O	300	5	72.6	0	0	0	18.4	0.6	8.4
Cu-ZSM5-0.3%	300	50	31.9	3.5	0.3	0.7	16.4	2.4	44.8
Cu-ZSM5-0.3%+20%H_2O	300	50	23.0	0.6	0	0	66.3	4.2	5.9

Table S2 Comparisons of CH_3OH productivity and selectivity for Cu-ZSM-0.3% and the other samples from reference

No.	Sample	method	CH_3OH productivity ($\mu mol \cdot g^{-1}_{cat} \cdot h^{-1}$)	CH_3OH selectivity (%)	CO_2 selectivity (%)	Refs.
1	Fe-ZSM-5-2.3%	incipient wetness impregnation	-	3.1	33	[1]
2	Fe-ZSM-5-1%F	freeze-drying	101.6	10.9	76.4 (CO_x)	[2]
3	Fe-ZSM-5-1%-E	incipient wetness impregnation	84.8	9.1	85.8 (CO_x)	[2]
4	Fe-ZSM-5-2.5%	chemical vapor impregnation	61.5	16	-	[3]
5	Fe-ZSM-5-2.0%	incipient wetness impregnation	72.3	62	49.5 (CO_x)	[4]
6	Cu-ZSM-5-4%	ion exchange	62	-	-	[5]
7	Cu-H-ZSM-5	ion exchange	1.81	-	-	[6]
8	Fe-ZSM-5-1.5%	chemical vapor impregnation	-	15.1	13.6	[7]
9	Cu-ZSM-5-1.5%	chemical vapor impregnation	-	89.1	9.9	[7]
10	Cu-ZSM-5-0.1%	solid-state ion exchange	81.7	9.9	15.3	
11	Cu-ZSM-5-0.3%	solid-state ion exchange	194.8	67.1	10.7	
12	Cu-ZSM-5-0.5%	solid-state ion exchange	131.5	31.2	53.2	This work
13	Cu-ZSM-5-0.8%	solid-state ion exchange	110.0	23.1	64.1	
14	Cu-ZSM-5-1.2%	solid-state ion exchange	108.0	18.4	72.6	

Reference

[1] G. Zhao, E. Benhelal, A. Adesina, E. Kennedy, M. Stockenhuber, Comparison of Direct, Selective Oxidation of Methane by N_2O over Fe-ZSM-5, Fe-Beta, and Fe-FER Catalysts, J. Phys. Chem. C, 123 (2019) 27436-27447.

[2] L. Fan, D.-g. Cheng, L. Song, F. Chen, X. Zhan, Direct Conversion of CH_4 to Oxy-organics by N_2O Using Freeze-drying FeZSM-5, Chem. Eng. J., 369 (2019) 522-528.

[3] Y.K. Chow, N.F. Dummer, J.H. Carter, R.J. Meyer, R.D. Armstrong, C. Williams, G. Shaw, S. Yacob, M.M. Bhasin, D.J. Willock, S.H. Taylor, G.J. Hutchings, A Kinetic Study of Methane Partial Oxidation over Fe-ZSM-5 Using N_2O as an Oxidant, Chem. Phys. Chem, 19 (2018) 402-411.

[4] M.V. Parfenov, E.V. Starokon, L.V. Pirutko, G.I. Panov, Quasicatalytic and Catalytic Oxidation of Methane to Methanol by Nitrous Oxide over FeZSM-5 Zeolite, J. Catal., 318 (2014) 14-21.

[5] V.L. Sushkevich, J.A. van Bokhoven, Methane-to-Methanol: Activity Descriptors in Copper-Exchanged Zeolites for the Rational Design of Materials, ACS Catal., 9 (2019) 6293-6304.

[6] K. Narsimhan, K. Iyoki, K. Dinh, Y. Roman-Leshkov, Catalytic Oxidation of Methane into Methanol over Copper-Exchanged Zeolites with Oxygen at Low Temperature, ACS Cent. Sci., 2 (2016) 424-429.

[7] J. Xu, R.D. Armstrong, G. Shaw, N.F. Dummer, S.J. Freakley, S.H. Taylor, G.J. Hutchings, Continuous Selective Oxidation of Methane to Methanol over Cu- and Fe-Modified ZSM-5 Catalysts in a Flow Reactor, Catal. Today, 270 (2016) 93-100.

Table S3 Elementary steps and kinetic parameters involved in microkinetic modeling over monomeric $[Cu]^+$ site during N_2O-DMTM in both presence and absence of H_2O.

Step	Elementary Step	Reaction rate equations	v_{for} (s^{-1})	v_{rev} (s^{-1})	ΔE (eV)	ΔE^{-1} (eV)
R1	Z-Cu □ N_2O(g) □ Z-Cu-N_2O	$r_1 = k_1 P_{N_2O} \theta_v - k_{-1} \theta_{N_2O}$	0.02	4.50×10^{18}	-	0.70
R2	Z-Cu-N_2O □ Z-Cu-O□ N_2(g)		2.53×10^{12}	-	1.41	-
R3	Z-Cu-O+CH_4 □ Z-Cu-OH-CH_3		4.61×10^{12}	4.18×10^{14}	0.09	4.54
R4	Z-Cu-OH-CH_3 □ Z-Cu-CH_3OH		3.59×10^{13}	8.73×10^{13}	0.34	1.38
R5	Z-Cu-CH_3OH □Z-Cu+CH_3OH(g)		4.70×10^{19}	-	1.45	-
R5’	Z-Cu-CH_3OH □$^{+H_2O}$□ Z-Cu+CH_3OH(g)		4.70×10^{19}	-	0.55	-

Table S4 Elementary steps and kinetic parameters involved in microkinetic modeling over dicopper $[Cu]^+$--$[Cu]^+$ site during N_2O-DMTM in both presence and absence of H_2O.

Step	Elementary Steps	Reaction rate equations	v_{for} (s^{-1})	v_{rev} (s^{-1})	ΔE (eV)	ΔE^{-1} (eV)
R1	$Z\text{-}Cu_2 + N_2O(g) \rightarrow Z\text{-}Cu_2\text{-}N_2O$	$r_1 = k_1 P_{N_2O} \theta_v - k_{-1} \theta_{N_2O}$	0.02	1.17×10^{21}	-	1.23
R2	$Z\text{-}Cu_2\text{-}N_2O \rightarrow Z\text{-}Cu_2\text{-}O + N_2(g)$	$r_2 = k_2 \theta_{N_2O}$	1.69×10^{13}	-	0.92	-
R3	$Z\text{-}Cu_2\text{-}O + CH_4(g) \rightarrow Z\text{-}Cu_2\text{-}CH_3\text{-}OH$	$r_3 = k_3 \theta_O P_{CH_4} - k_{-3} \theta_{CH_3OH}$	2.25×10^{11}	1.07×10^{13}	0.71	0.73
R4	$Z\text{-}Cu_2\text{-}CH_3\text{-}OH \rightarrow Z\text{-}Cu_2\text{-}CH_3OH$	$r_4 = k_4 \theta_{CH_3\text{-}OH} - k_{-4} \theta_{CH_3OH}$	7.70×10^{12}	4.72×10^{13}	0.08	1.06
R5	$Z\text{-}Cu_2\text{-}CH_3OH \rightarrow Z\text{-}Cu_2 + CH_3OH(g)$	$r_5 = k_5 \theta_{CH_3OH}$	9.77×10^{21}	-	2.02	-
R5’	$Z\text{-}Cu_2\text{-}CH_3OH \xrightarrow{H_2O} Z\text{-}Cu + CH_3OH(g)$	$r_5 = k_5 \theta_{CH_3OH}$	9.77×10^{21}	-	0.01	-